A Novel Augmented Subspace Adaptive Finite Element Method for the Eigenvalue Problem with Discontinuous Coefficients

Manting Xie* and Meiling Yue†

Abstract

This paper proposes an efficient Adaptive Finite Element Method (AFEM) for solving the eigenvalue problem with *discontinuous coefficients*. Different from the existing adaptive algorithms for eigenvalue problems, the method innovatively focuses on solving linearized boundary value problems in each adaptively refined space, complemented by solving small-scale eigenvalue problems on low-dimensional augmented subspaces, which are automatically controlled by the algorithm. Notably, it does not require solving the small-scale eigenvalue problem at every iteration, which improves the computational efficiency. Moreover, a novel a posteriori error estimator, which relies on the local oscillations of coefficients near singular points, guides the adaptive refinement process. To further substantiate this method, we give a thorough and rigorous convergence analysis in this paper. Finally, two numerical examples are provided to illustrate the accuracy and efficiency of our new AFEM.

Keywords. Eigenvalue problem; discontinuous coefficient; adaptive finite element method; augmented subspace method.

AMS subject classifications. 65N30, 65N25, 65L15, 65B99.

1 Introduction

Solving large-scale eigenvalue problems becomes a fundamental problem in modern science and engineering society. Eigenvalue problems with discontinuous coefficients [29, 39] arise in various applications, including photonic crystals and their spectral band gaps [6, 15, 44], Sturm-Liouville equation and inverse eigenvalue problems [1, 5, 18], and quantum physics [9, 21] et al. In recent years, a few numerical investigations have been devoted to computing eigenvalue problems with discontinuous coefficients, such as the plane wave expansion method [23], finite element method [6,40], spectral (element) method [29, 39], two-grid method [10], discontinuous Galerkin method [8, 26]. However, those direct applications of standard discretization schemes lead to particularly high computational costs. In fact, discontinuous coefficients across the interface can lead to abrupt changes in the solution, exhibiting inherent multiscale behavior characterized by localized high-gradient zones near the interface.

Subspace correction methods [42] are a fundamental and effective class of algorithms for eigenvalue problems. The two-grid/two-level method has proven to be an efficient numerical approach. Since its initial development by Xu and Zhou [43], this approach has inspired subsequent advancements in [14, 19], particularly in addressing challenging eigenvalue problems with nonlinearity. Additionally, [4] proposed a polynomial-based subspace correction approach with guaranteed superconvergence. Recently, a type of efficient augmented subspace method (multigrid or multilevel correction method) for eigenvalue problems has been proposed in Ref. [22, 24, 41]. In particular, this augmented subspace method can achieve the optimal error estimate with (quasi-)optimal computational work.

The adaptive mesh refinement method based on the a posteriori error estimator has been widely used to improve the convergence rate of the singular problem [9, 21, 37]. Based on the augmented subspace method, [20] has proposed h-adaptive multilevel methods for eigenvalue problems. Furthermore,

*School of Mathematics and KL-AAGDM, Tianjin University, Tianjin, 300350, China (mtxie@tju.edu.cn)

†Corresponding Author. School of Mathematics and Statistics, Beijing Technology and Business University, Beijing 100048, China (yuemeiling@lsec.cc.ac.cn)

several effective p-adaptive methods (achieving accuracy enhancement through polynomial order adjustment) have been proposed for eigenvalue problems in references [4, 16, 17, 33]. In particular, the adaptive finite element method (AFEM) has been successfully applied to photonic crystal eigenvalue problems (a class of eigenvalue problems with discontinuous coefficients) [15,36]. For eigenvalue problems with discontinuous coefficients, [34,35] have developed effective a posteriori error estimators. To the best of our knowledge, rigorous convergence proofs for AFEM applied to eigenvalue problems with discontinuous coefficients remain scarce in the literature.

In this paper, we propose a new type of augmented subspace AFEM to solve eigenvalue problems with discontinuous coefficients. Overall, the main objectives of this paper are threefold:

(1) Adopt the a posteriori error estimator $\eta(f, u_h; e)$ of *the linearized boundary value problem* with discontinuous coefficients for the discussed eigenvalue problem

$$\eta^2(f, u_h; e) = \sum_{\tau \in \omega_e} \Lambda_\tau \|h_\tau \alpha_\tau^{-1/2} \mathcal{R}_\tau(f, u_h)\|_{0,\tau}^2 + \Lambda_e \|h_e^{1/2} \alpha_e^{-1/2} \mathcal{J}_e(u_h)\|_{0,e}^2,$$

where f is the right-hand side of the linearized boundary value problem, u_h is the approximation of the eigenfunction on the discussed mesh; e is the edge of the element, ω_e is the collection of two elements sharing the edge e, h_τ and h_e are the diameter of element τ and edge e, respectively; $\mathcal{R}_\tau(f, u_h)$ is the element residual, $\mathcal{J}_e(u_h)$ is the jump residual; Λ_τ, Λ_e, α_τ and α_e are constants related to the coefficient α. Please see (3.1) for details.

(2) Develop a new AFEM solver (Algorithm 3.3 and the flowchart Fig. 1) for eigenvalue problems with discontinuous based on the augmented subspace method, which is accelerated by the inverse power method.

(3) Derive the convergence (Theorem 4.2) of the proposed augmented subspace AFEM algorithm for eigenvalue problems with discontinuous coefficients.

In this algorithm, we try to *balance* the linear error (the numerical error of the linearized boundary value problem) and the nonlinear error (the error between the solutions of the eigenvalue problem and the corresponding linearized boundary value problem) to ensure error reduction while reducing computational costs. More precisely (cf. Step 3 of Algorithm 3.2),

(a) if the linear error is *larger* than the nonlinear error in some sense, we refine the mesh adaptively and solve the linearized boundary value problem (the inverse power method) defined on the adaptively refined mesh to reduce the linear error;

(b) otherwise, we solve the small-scale eigenvalue problem on the low-dimensional augmented subspace $V_H + \text{span}\{u_h^{(j)}\}$ and update the right-hand side term of the linearized boundary value problem to reduce the nonlinear error,

here V_H is the finite element space defined on the coarsest mesh. The initial mesh for our adaptive finite element method can be either V_H or a uniform refinement of V_H. The term $u_h^{(j)}$ represents the approximate solution of the corresponding boundary value problem, please see Algorithm 3.2 for details.

Actually, we can prove that the nonlinear error is a higher-order term compared with the linear error and the higher-order factor is $\zeta_a(V_H)$ defined in (2.8), see Lemma 3.5 and Theorem 4.1 for details. Therefore, we mainly focus on solving the linearized boundary value problems defined on adaptively refined meshes to reduce the linear error. Since the main computational work is spent on solving the linearized boundary value problems, the cost of this AFEM can be improved to be almost the same as that of the associated linearized boundary value problems. Compared with [20], our method greatly reduces the number of eigenvalue problems solved on augmented subspaces, thereby improving the computational efficiency. For details, please refer to Tables 1 and 2 in the numerical experiments.

The rest of this paper goes as follows. The considered eigenvalue problem and its corresponding finite element method are given in Section 2. In Section 3, the efficient augmented subspace AFEM is proposed for the eigenvalue problem with discontinuous coefficients. We give the analysis of the convergence of our AFEM algorithm in Section 4. Two numerical examples are presented in Section 5 to illustrate the efficiency of the proposed AFEM algorithm. In the last section, we give some concluding remarks.

2 Finite element method for eigenvalue problems with discontinuous coefficients

We use the standard notation for Sobolev spaces $W^{s,p}(\Omega)$ and their associated norms (cf. [12]). We denote $H^1(\Omega) = W^{1,2}(\Omega)$ equipped with the norm $\|\cdot\|_1$. Let $H_0^1(\Omega) = \{v \in H^1(\Omega) : v|_{\partial\Omega} = 0\}$, where $v|_{\partial\Omega}$ is understood in the sense of trace. For simplicity, we denote $V := H_0^1(\Omega)$. In this paper, the notation $A \lesssim B$ means that $A \le CB$ for some constant C which is independent of the mesh size.

2.1 Eigenvalue problems with discontinuous coefficients

In this subsection, we shall present some basic results of the finite element method for the second-order elliptic eigenvalue problem. Here, for simplicity, we are concerned with the following general eigenvalue problem with discontinuous coefficients:

$$\begin{cases} \mathcal{L}u := -\nabla\cdot(\alpha(\boldsymbol{x})\nabla u) + \varphi(\boldsymbol{x})u &= \lambda u \quad \text{in } \Omega, \\ u &= 0 \quad \text{on } \partial\Omega, \\ \int_\Omega |u|^2 \mathrm{d}\Omega &= 1, \end{cases} \tag{2.1}$$

where Ω is a polyhedral domain in $\mathbb{R}^d$ $(d = 2, 3)$, the discontinuous coefficient $\alpha(\boldsymbol{x})$ is positive and piecewise constant and $0 \le \varphi(\boldsymbol{x}) \in L^\infty(\Omega)$.

The weak form for (2.1) is defined as follows: Find $(\lambda, u) \in \mathbb{R} \times V$ such that $\|u\|_b = 1$ and

$$a(u, v) = \lambda b(u, v), \quad \forall v \in V, \tag{2.2}$$

where the bounded bilinear form $a(\cdot,\cdot)$ and $b(\cdot,\cdot)$ are defined by

$$a(u, v) = \int_\Omega (\alpha\nabla u\cdot\nabla v + \varphi uv)\mathrm{d}\Omega, \quad b(u, v) = \int_\Omega uv\mathrm{d}\Omega, \tag{2.3}$$

respectively, and $\|\cdot\|_b := \sqrt{b(\cdot,\cdot)}$. It is evident that $\|\cdot\|_b$ is nothing but the standard norm $\|\cdot\|_{L^2(\Omega)}$.

From properties of $\alpha(\boldsymbol{x})$ and $\varphi(\boldsymbol{x})$, the bilinear form $a(\cdot,\cdot)$ satisfies

$$|a(w, v)| \lesssim \|w\|_1\|v\|_1, \quad \forall\, w, v \in V,$$
$$\|w\|_1^2 \lesssim a(w, w), \quad \forall\, w \in V.$$

Hence we can define the energy norm as $\|\cdot\|_a = \sqrt{a(\cdot,\cdot)}$, then we have

$$c_a\|v\|_1 \le \|v\|_a \le C_a\|v\|_1, \quad \forall\, v \in V,$$

where c_a and C_a are some positive constants. Hence, we have the following inequality between $\|\cdot\|_b$ and $\|\cdot\|_a$,

$$\|v\|_b \le \|v\|_1 \le \frac{1}{c_a}\|v\|_a, \quad \forall\, v \in V. \tag{2.4}$$

Define the Rayleigh quotient as

$$RQ(v) := \frac{a(v, v)}{b(v, v)}, \quad \forall\, v \in V\backslash\{0\}.$$

As we know, the eigenvalue problem (2.2) has a countable sequence of real eigenvalues

$$0 < \lambda_1 < \lambda_2 \le \lambda_3 \le \cdots$$

and corresponding orthogonal eigenfunctions

$$u_1, u_2, u_3, \ldots,$$

which satisfy $b(u_i, u_j) = \delta_{ij}$ $(i, j = 1, 2, \ldots)$, where δ_{ij} is the Kronecker notation. In the sequence $\{\lambda_i\}_{i\ge1}$, the λ_i are repeated q times according to their geometric multiplicity q.

Now we state a useful Rayleigh quotient expansion for an eigenvalue, which is expressed by the eigenfunction approximation (see [3]).

Lemma 2.1. *Let (λ, u) be an eigenpair of (2.2). Then for any $w \in V\backslash\{0\}$, we have*

$$\frac{a(w, w)}{b(w, w)} - \lambda = \frac{a(w - u, w - u)}{b(w, w)} - \frac{\lambda b(w - u, w - u)}{b(w, w)}. \tag{2.5}$$

2.2 Finite element method for eigenvalue problems with discontinuous coefficients

In this subsection, we introduce the finite element method for problem (2.2). We first decompose the computing domain $\Omega \subset \mathbb{R}^2$ into triangles to produce the mesh such that $\alpha(\boldsymbol{x})$ is a constant on the interior point of each element (cf. [12]). In this paper, we discuss the finite element discretization on a family of shape-regular and nested conforming meshes $\mathbb{T} := \{\mathcal{T}_h\}_{h>0}$: there exists a constant γ^* such that

$$\frac{h_\tau}{h'_\tau} \leq \gamma^*, \qquad \forall\, \tau \in \bigcup_h \mathcal{T}_h,$$

where h_τ is the diameter of τ for each element $\tau \in \mathcal{T}_h$, h'_τ is the diameter of the biggest ball contained in τ and $h := \max\{h_\tau : \tau \in \mathcal{T}_h\}$. $\mathcal{E}_h$ is used to denote the set of interior edges of $\mathcal{T}_h$. For any $e \in \mathcal{E}_h$, we denote the diameter by h_e. For any $\tau \in \mathcal{T}_h$, let $\omega_\tau = \left\{\tau' \in \mathcal{T}_h \ : \ \overline{\tau'} \cap \overline{\tau} \neq \emptyset\right\}$. Let ω_e be the collection of two elements sharing the edge $e \in \mathcal{E}_h$.

For each node x, let ω_x be the union of all elements τ sharing x as the common node, and let κ_x be all elements $\tau \subset \omega_x$ where the coefficients α_τ achieve the maximum in ω_x. The distribution of coefficients $\alpha_\tau,\ \tau \subset \omega_x$, will be called quasi-monotone with respect to x if the following conditions are fulfilled: For each element $\tau \subset \omega_x$ there exists a Lipschitz set $\tau_x^{\rm qm}$ with $(\tau \cup \kappa_x) \subset \tau_x^{\rm qm} \subset \omega_x$, such that

$$\alpha_\tau \leq \alpha_{\tau'}, \quad \forall \tau' \subset \tau_x^{\rm qm}, \quad \tau' \in \mathcal{T}_h.$$

If x is a boundary node, it is additionally required that ${\rm meas}_{d-1}(\partial\tau_x^{\rm qm} \cap \partial\Omega) > 0$. The nodes concerning which the quasi-monotone condition is violated are called **singular nodes**. For further information about the quasi-monotone condition, we refer to [13].

Then the conforming finite element space $V_h \subset V$ can be constructed based on the mesh $\mathcal{T}_h$. For simplicity, we consider the Lagrange-type finite element space

$$V_h = \left\{v_h \in V \ : \ v_h|_\tau \in \mathcal{P}_m(\tau), \ \ \forall \tau \in \mathcal{T}_h\right\},$$

where $\mathcal{P}_m(\tau)$ denotes the space of polynomials with degree no more than m.

The standard finite element scheme for (2.2) is: Find $(\lambda_h, u_h) \in \mathbb{R} \times V_h$ such that $b(u_h, u_h) = 1$ and

$$a(u_h, v_h) = \lambda_h b(u_h, v_h), \ \ \forall\, v_h \in V_h. \tag{2.6}$$

From Ref. [2,3], we know that the discrete eigenvalue problem (2.6) has eigenvalues

$$0 < \lambda_{1,h} \leq \cdots \leq \lambda_{i,h} \leq \cdots \leq \lambda_{N_h,h},$$

and corresponding eigenfunctions

$$u_{1,h}, \cdots, u_{i,h}, \cdots, u_{N_h,h},$$

where $b(u_{i,h}, u_{j,h}) = \delta_{ij}$, $1 \leq i, j \leq N_h$ (N_h is the dimension of the finite element space V_h).

Based on the finite element space V_h, the Galerkin-Ritz projection $P_h : V \to V_h$ can be defined by

$$a(w - P_h w, v_h) = 0, \ \ \forall w \in V \text{ and } \forall v_h \in V_h. \tag{2.7}$$

Then, it is easy to know, for any $w \in V$

$$\|P_h w\|_a \leq \|w\|_a \text{ and } \|w - P_h w\|_a \to 0, \text{ as } h \to 0.$$

Define $\zeta_a(V_h)$ as

$$\zeta_a(V_h) := \sup_{f \in L^2(\Omega), \|f\|_b = 1} \inf_{v_h \in V_h} \|Tf - v_h\|_a, \tag{2.8}$$

where the operator $T : L^2(\Omega) \to V$ is defined by the following boundary value problem: for any $f \in L^2(\Omega)$, find $w \in V$, such that

$$a(w, v) = b(f, v), \ \ \forall v \in V, \tag{2.9}$$

and $Tf := w$.

Let $M(\lambda_i)$ denote the eigenspace corresponding to the eigenvalue λ_i of (2.2), i.e.,

$$M(\lambda_i) = \big\{w \in V : w \text{ is an eigenfunction of (2.2) corresponding to } \lambda_i\big\}.$$

To simplify the description, we define the following error notation:

$$\delta_h(\lambda_i) := \sup_{w \in M(\lambda_i), \|w\|_b = 1} \inf_{v_h \in V_h} \|w - v_h\|_a.$$

From Ref. [2,3], we know that $\zeta_a(V_h)$, $\delta_h(\lambda_i) \to 0$, as $h \to 0$ and

$$\zeta_a(V_h') \le \zeta_a(V_h), \text{ if } V_h \subset V_h'. \tag{2.10}$$

The error estimates of the eigenpair approximations for the eigenvalue problem with discontinuous coefficients by the finite element method is stated in the following theorem.

Theorem 2.1 ([2,15]). *Assume $(\lambda_{i,h}, u_{i,h}) \in \mathbb{R} \times V_h$ is the solution of (2.6). Then there exists exact eigenpair (λ_i, u_i) of (2.2) such that the following error estimates hold*

$$\begin{aligned} \|u_{i,h} - u_i\|_a &\le C_{ea}\delta_h(\lambda_i), \\ \|u_{i,h} - u_i\|_b &\le C_{eb}\zeta_a(V_h)\|u_{i,h} - u_i\|_a, \\ |\lambda_{i,h} - \lambda_i| &\le C_{e\lambda}\|u_{i,h} - u_i\|_a^2 \le C_{e\lambda}\delta_h(\lambda_i)\|u_{i,h} - u_i\|_a, \end{aligned}$$

where C_{ea}, C_{eb} and $C_{e\lambda}$ are some positive constants independent of the mesh size h.

Remark 2.1. *It should be noted that $\zeta_a(V_h)$ is essentially the higher-order factor of the convergence analysis from $\|\cdot\|_a$ (H^1-norm) to $\|\cdot\|_b$ (L^2-norm) in the Aubin-Nitsche duality argument.*

3 Augmented subspace AFEM for eigenvalue problems with discontinuous coefficients

We now give a new AFEM algorithm based on the augmented subspace method for eigenvalue problems with discontinuous coefficients. More details about the augmented subspace method can be found in Ref. [24, 41]. At first, we recall the classical AFEM for the boundary value problem. For simplicity, we omit the subscript i of the eigenpair (λ_i, u_i) and approximation solution $(\lambda_{i,h}, u_{i,h})$ hereafter.

3.1 AFEM for boundary value problem

For problem (2.9), given the initial mesh, the form of the standard AFEM can be described as

$$\mathsf{SOLVE} \to \mathsf{ESTIMATE} \to \mathsf{MARK} \to \mathsf{REFINE}.$$

Considering the discontinuous coefficient for the boundary value problem, we use a kind of error estimator that depends locally on the oscillations of the coefficients around singular points. For a right hand side term $f \in L^2(\Omega)$ and a finite element function $v_h \in V_h$, we define the element residual $\mathcal{R}_\tau(f, v_h)$ and the jump residual $\mathcal{J}_e(v_h)$ as follows

$$\begin{aligned} \mathcal{R}_\tau(f, v_h) &:= f - \mathcal{L}v_h = f + \nabla \cdot (\alpha \nabla v_h) - \varphi v_h, \quad \text{in } \tau \in \mathcal{T}_h, \\ \mathcal{J}_e(v_h) &:= -(\alpha \nabla v_h^+) \cdot \boldsymbol{n}^+ - (\alpha \nabla v_h^-) \cdot \boldsymbol{n}^- = [\![\alpha \nabla v_h]\!]_e \cdot \boldsymbol{n}_e, \quad \text{on } e \in \mathcal{E}_h, \end{aligned}$$

where $u_h^+ = u_h|_{\tau^+}, u_h^- = u_h|_{\tau^-}$, e is the common edge of element τ^+ and τ^- with the unit outward normals $\boldsymbol{n}^+$ and $\boldsymbol{n}^-$, respectively and $\boldsymbol{n}_e = \boldsymbol{n}^+$. For the problem with discontinuous coefficients, we introduce the following modified local residual estimator $\eta(f, u_h; e)$ [11]

$$\eta^2(f, v_h; e) := \sum_{\tau \in \omega_e} \Lambda_\tau \|h_\tau \alpha_\tau^{-1/2} \mathcal{R}_\tau(f, v_h)\|_{0,\tau}^2 + \Lambda_e \|h_e^{1/2} \alpha_e^{-1/2} \mathcal{J}_e(v_h)\|_{0,e}^2, \tag{3.1}$$

where $\|\cdot\|_{0,\tau}$ and $\|\cdot\|_{0,e}$ denote the standard L^2-norm on element τ and edge e, respectively, and α_τ is the constant value of $\alpha(\boldsymbol{x})$ on interior point of $\tau \in \mathcal{T}_h$, $\alpha_e := \max_{\tau\in\omega_e}\{\alpha_\tau\}$ for $e \in \mathcal{E}_h$,

$$\Lambda_\tau := \begin{cases} \max\limits_{\tau'\in\omega_\tau}\left(\dfrac{\alpha_\tau}{\alpha_{\tau'}}\right), & \text{if } \tau \text{ has one singular node,} \\ 1, & \text{otherwise,} \end{cases}$$

where $\Lambda_e := \max\limits_{\tau\in\omega_e}\{\Lambda_\tau\}$.

For any submesh $\mathcal{T}_h' \subset \mathcal{T}_h$, we denote interior edges of $\mathcal{T}_h'$ by $\mathcal{E}_h'$, and define

$$\eta^2(f, v_h; \mathcal{T}_h') := \sum_{e\in\mathcal{E}_h'} \eta^2(f, v_h; e). \tag{3.2}$$

For any $f \in L^2(\Omega)$, we define the local data oscillation as

$$\mathrm{osc}^2(f, v_h; \tau) := \|h_\tau \alpha_\tau^{-1/2}(I - Q_\tau)\mathcal{R}_\tau(f, v_h)\|_{0,\tau}^2, \tag{3.3}$$

where Q_τ is the L^2 projection operator onto polynomials of some degree on τ. For any submesh $\mathcal{T}_h' \subset \mathcal{T}_h$, we define data oscillation as

$$\mathrm{osc}^2(f, v_h; \mathcal{T}_h') := \sum_{\tau\in\mathcal{T}_h'} \mathrm{osc}^2(f, v_h; \tau).$$

Now, we present the reliability and efficiency of the a posteriori error estimator $\eta(f, P_h w; \mathcal{T}_h)$ for boundary value problem (2.9) in the following lemma (see, e.g. [11, 28, 31]).

Lemma 3.1 ([11, Theorem 2.1, Theorem 2.2])**.** *For any $f \in L^2(\Omega)$, there exist constant C_{up} only depending on the regularity constant γ^* and the coercivity constant c_a, and the constant C_{low} only depending on γ^* and the continuity constant C_a such that*

$$\|(I - P_h)Tf\|_a \leq C_{\mathrm{up}}\eta(f, P_hTf; \mathcal{T}_h), \tag{3.4}$$

$$C_{\mathrm{low}}\eta(f, P_hTf; \mathcal{T}_h) \leq \Lambda^{\frac{1}{2}}\big(\|(I - P_h)Tf\|_a + \mathrm{osc}(f, P_hTf; \mathcal{T}_h)\big), \tag{3.5}$$

where $\Lambda = \max\limits_{\tau\in\mathcal{T}_h}\{\Lambda_\tau\}$, and Tf is the solution of problem (2.9).

For convenience, we define some modules to present the standard AFEM algorithm for the boundary value problem.

- $w_h = \mathsf{B\_SOLVE}(f, V_h)$: Solve the *boundary* value problem (2.9) with the right-hand side term f in the finite element space V_h and output the approximate solution $w_h \in V_h$.
- $\big[\{\eta(f, v_h; e)\}, \{\mathrm{osc}(f, v_h; \tau)\}\big] = \mathsf{ESTIMATE}(f, v_h, \mathcal{T}_h)$: Compute the error indicator on each interior edge $e \in \mathcal{E}_h$ of $\mathcal{T}_h$ according to (3.1) and the data oscillation on each element $\tau \in \mathcal{T}_h$ according to (3.3).
- $\mathcal{M}_h = \mathsf{MARK}\big(\theta_1, \widehat{\theta}_1, \{\eta(f, v_h; e)\}, \{\mathrm{osc}(f, v_h; \tau)\}, \mathcal{T}_h\big)$: Construct a subset $\mathcal{M}_h$ of $\mathcal{T}_h$ by **Morin-Nochetto-Siebert (MNS)-marking strategy** (c.f. [30]) with θ_1, $\widehat{\theta}_1 \in (0, 1)$, $(f, v_h, \mathcal{T}_h)$, and mark all elements in $\mathcal{M}_h$.
- $[\mathcal{T}_{h_{k+1}}, V_{h_{k+1}}] = \mathsf{REFINE}(\mathcal{M}_{h_k}, \mathcal{T}_{h_k})$: Output a conforming refinement $\mathcal{T}_{h_{k+1}}$ of $\mathcal{T}_{h_k}$ where at least all element in $\mathcal{M}_{h_k}$ are refined and construct the corresponding finite element space $V_{h_{k+1}}$ on $\mathcal{T}_{h_{k+1}}$.

Remark 3.1. *We use the iterative or recursive bisection (see, e.g. [27, 38]) of elements with the minimal refinement condition in* REFINE*. Let $\gamma \in (0, 1)$ be the reduction factor of element size associated with one refinement step, then if τ' is one of the elements obtained by refining τ once, we have $h_{\tau'} \leq \gamma h_\tau$ (c.f. [11, Lemma 3.3] and [30, Lemma 3.8]).*

For ease of reference, we now recall the MNS-marking strategy in Ref. [30].

MNS-marking strategy

Input: $\theta_1, \widehat{\theta}_1 \in (0,1)$, $\mathcal{T}_h \in \mathbb{T}$, $f \in L^2(\Omega)$ and $v_h \in V_h$.

Marking strategy:

1. Select a subset $\widehat{\mathcal{E}}_h$ of sides in $\mathcal{E}_h$ such that

$$\left(\sum_{e\in\widehat{\mathcal{E}}_h} \eta^2(f, v_h; e)\right)^{1/2} \geq \theta_1 \left(\sum_{e\in\mathcal{E}_h} \eta^2(f, v_h; e)\right)^{1/2}.$$

2. Let $\mathcal{M}_h$ be the set of elements with one side in $\widehat{\mathcal{E}}_h$. Enlarge $\mathcal{M}_h$ such that

$$\mathrm{osc}(f, v_h; \mathcal{M}_h) \geq \widehat{\theta}_1 \mathrm{osc}(f, v_h; \mathcal{T}_h).$$

Output: $\mathcal{M}_h \subset \mathcal{T}_h$.

Then we recall the standard AFEM for the boundary value problem (2.9).

Algorithm 3.1. ***AFEM for boundary value problem***

Input: *Given some parameters* $\theta_1, \widehat{\theta}_1 \in (0,1), \varepsilon > 0$, *a function* $f \in L^2(\Omega)$, *a mesh* $\mathcal{T}_{h_1} \in \mathbb{T}$ *and the corresponding finite element space* V_{h_1}.

Iteration: *Set* $k = 1$ *and do the following loops:*

1. $w_{h_k} = \mathsf{B\_SOLVE}(f, V_{h_k})$;

2. $\big[\{\eta(f, w_{h_k}; e)\}, \{\mathrm{osc}(f, w_{h_k}; \tau)\}\big] = \mathsf{ESTIMATE}(f, w_{h_k}, \mathcal{T}_{h_k})$;

3. **if** $\eta(f, w_{h_k}; \mathcal{T}_{h_k}) < \varepsilon$
   return w_{h_k};
   else
   $\mathcal{M}_{h_k} = \mathsf{MARK}\big(\theta_1, \widehat{\theta}_1, \{\eta(f, w_{h_k}; e)\}, \{\mathrm{osc}(f, w_{h_k}; \tau)\}, \mathcal{T}_{h_k}\big)$;

4. $[\mathcal{T}_{h_{k+1}}; V_{h_{k+1}}] = \mathsf{REFINE}(\mathcal{M}_{h_k}, \mathcal{T}_{h_k})$;

5. *Set* $k = k + 1$ *and* **goto** *Step 1.*

Output: *The approximate solution* w_{h_k}.

For the finite element solution of the boundary value problem (2.9), it is easy to know

$$w_{h_k} = P_{h_k} w = P_{h_k} T f$$

based on (2.7). About the AFEM Algorithm 3.1 for boundary value problems, we state the following three lemmas.

Lemma 3.2 ([11, Lemma 3.2])**.** *Let* $\mathcal{T}_{h_{k+1}}$ *be a refinement of* $\mathcal{T}_{h_k}$ *according to the MNS-marking strategy,* $w_{h_{k+1}}$ *and* w_{h_k} *are the finite element solution on the mesh* $\mathcal{T}_{h_{k+1}}$ *and* $\mathcal{T}_{h_k}$*, respectively. Then*

there exists a constant $\widetilde{C}_{\text{low}} \leq 1$ *depending only on the minimum angle of the mesh* $\mathcal{T}_{h_k}$ *such that for all* $e \in \widehat{\mathcal{E}}_{h_k}$ *(the collection of all sides belonging to the marked elements) we have*

$$\widetilde{C}_{\text{low}}\eta(f, w_{h_k}; e) \leq \Lambda_e^{\frac{1}{2}} \left(\sum_{\tau \in \omega_e} \|w_{h_{k+1}} - w_{h_k}\|_{a,\tau} + \sum_{\tau \in \omega_e} \text{osc}(f, w_{h_k}; \tau) \right).$$

Here we recall that $\Lambda_e = \max_{\tau \in \omega_e}\{\Lambda_\tau\}$.

Lemma 3.3 ([11, Lemma 3.3])**.** *Given the refine parameter* $\widehat{\theta}_1 \in (0,1)$*, let* $\widehat{\sigma} = \left(1 - (1-\gamma^2)\widehat{\theta}_1^2\right)^{\frac{1}{2}}$ *and* $\mathcal{T}_{h_{k+1}}$ *be a refinement of* $\mathcal{T}_{h_k}$ *according to MNS-marking strategy. Then we have*

$$\text{osc}(f, w_{h_{k+1}}; \mathcal{T}_{h_{k+1}}) \leq \widehat{\sigma}\text{osc}(f, w_{h_k}; \mathcal{T}_{h_k}).$$

Lemma 3.4 ([11, Theorem 3.4])**.** *Let* $\beta \in \mathbb{R}$ *satisfy* $\max\{\sigma, \widehat{\sigma}\} < \beta < 1$ *where*

$$\sigma = \left(1 - \frac{\widetilde{C}_{\text{low}}^2 \theta_1^2}{2C_{\text{up}}^2 \Lambda}\right)^{1/2},$$

here $\widetilde{C}_{\text{low}} \leq 1$ *is defined in Lemma 3.2,* $\Lambda := \max_{\tau \in \mathcal{T}_{h_k}} \Lambda_\tau$*, and* $\widehat{\sigma}$ *is defined in Lemma 3.3. Set*

$$C_0 = \left(\|(I - P_{h_1})w\|_a^2 + \frac{1}{\beta^2 - \min\{\sigma^2, \widetilde{\sigma}^2\}} \text{osc}^2(f, w_{h_1}; \mathcal{T}_{h_1}) \right)^{1/2}.$$

Then, the AFEM Algorithm 3.1 for boundary value problem produce a convergent sequence $\{w_{h_k}\}_{k \geq 1}$ *of discrete solutions such that*

$$\|(I - P_{h_k})w\|_a \leq C_0 \beta^{(k-1)}. \tag{3.6}$$

3.2 Augmented subspace AFEM for eigenvalue problems with discontinuous coefficients

Based on the augmented subspace method, we need to solve both the boundary value problem and the eigenvalue problem in the proposed AFEM algorithm. Then we introduce the following module.

- $(\lambda_h, u_h) =$ E_SOLVE(V_h): Solve the eigenvalue problem (2.6) in the finite element space V_h and output the desired discrete eigenpair $(\lambda_h, u_h) \in \mathbb{R} \times V_h$.

3.2.1 Iterative augmented subspace method

To describe the augmented subspace AFEM algorithm for eigenvalue problems with discontinuous coefficients clearly, we first give the iterative augmented subspace method in this subsection.

We first choose the coarsest mesh $\mathcal{T}_H$ on Ω, and then construct the corresponding Lagrange-type finite element space V_H as

$$V_H = \left\{ v_H \in V \ : \ v_H|_\tau \in \mathcal{P}_m(\tau), \ \ \forall \tau \in \mathcal{T}_H \right\}.$$

Suppose we are given a refined finite element space V_h ($V_H \subset V_h$), a parameter $\theta_2 \in (0,1)$ and a function $f_h^{(0)} \in L^2(\Omega)$. Assume $\zeta > 0$ is a given error indicator (see Algorithm 3.3 for details), the iterative augmented subspace method is defined by Algorithm 3.2.

Algorithm 3.2. ***Iterative augmented subspace method***

Input: *Given a parameter* $\theta_2 \in (0,1)$*, a function* $f_h^{(0)} \in L^2(\Omega)$*, an error indicator* $\zeta > 0$*, a coarse finite element space* V_H *and a refined finite element space* V_h*.*

Iteration: *Set* $j = 0$ *and do the following loops:*

1. $u_h^{(j)} = \mathsf{B\_SOLVE}(f_h^{(j)}, V_h)$, $\lambda_h^{(j)} = RQ(u_h^{(j)})$;

2. $\big[\{\eta(f_h^{(j)}, u_h^{(j)}; e)\}, \{\mathrm{osc}(f_h^{(j)}, u_h^{(j)}; \tau)\}\big] = \mathsf{ESTIMATE}(f_h^{(j)}, u_h^{(j)}, \mathcal{T}_h)$;

3. *(a)* **if** $\eta(f_h^{(j)}, u_h^{(j)}; \mathcal{T}_h) > \theta_2^{j+1}\zeta$

return $\big(\lambda_h^{(j)}, u_h^{(j)}, \{\eta(f_h^{(j)}, u_h^{(j)}; e)\}, \{\mathrm{osc}(f_h^{(j)}, u_h^{(j)}; \tau)\}, j\big)$;

(b) **else**

$(\widetilde{\lambda}_h^{(j)}, \widetilde{u}_h^{(j)}) = \mathsf{E\_SOLVE}(V_H + \mathrm{span}\{u_h^{(j)}\})$, $f_h^{(j+1)} = \widetilde{\lambda}_h^{(j)}\widetilde{u}_h^{(j)}$, $j = j+1$,

goto *Step 1.*

Output: *The eigenpair approximation* $(\lambda_h^{(j)}, u_h^{(j)})$, *estimator* $\{\eta(f_h^{(j)}, u_h^{(j)}; e)\}$, *oscillation* $\{\mathrm{osc}(f_h^{(j)}, u_h^{(j)}; \tau)\}$ *and the maximum value of iteration indicator* j;

Denote this augmented subspace method as

$$\big[(\lambda_h, u_h), \{\eta(f_h, u_h; e)\}, \{\mathrm{osc}(f_h, u_h; \tau)\}, j_h\big] = \mathbf{IterAugSub}(\theta_2, V_H, V_h, \zeta, f_h^{(0)}).$$

It should be noted that the maximum value j_h of the iteration index j exists. Please refer to Remark 3.3 for details.

Remark 3.2. *In practical implementation, for the eigenvalue problem defined in the augmented subspace* $V_H + \mathrm{span}\{u_h^{(j)}\}$, *we choose the one with the largest component on* $u_h^{(j)}$ *as the eigenfunction approximation* $\widetilde{u}_h^{(j)}$ *to make sure we obtain the desired eigenpair.*

According to Algorithm 3.2, define the corresponding solution of the boundary value problem

$$w^{(j)} := T f_h^{(j)},\ j = 0, \cdots, j_h, \tag{3.7}$$

then we have

$$u_h^{(j)} = P_h T f_h^{(j)} = P_h w^{(j)},\ j = 0, \cdots, j_h. \tag{3.8}$$

Together with (3.7)-(3.8) and the triangle inequality, we give the following inequality

$$\|u_h^{(j)} - u\|_a \le \|(I - P_h)w^{(j)}\|_a + \|w^{(j)} - u\|_a,\ j = 0, \cdots, j_h. \tag{3.9}$$

Actually, $\|(I - P_h)w^{(j)}\|_a$ is the *linear error* (the numerical error of the linearized boundary value problem) and $\|w^{(j)} - u\|_a$ denotes the *nonlinear error* (the error between solutions of the linearized boundary value problem and eigenvalue problem). Furthermore, the following lemma shows that the nonlinear error $\|w^{(j)} - u\|_a$ is a higher-order term.

Lemma 3.5. *Suppose* $w^{(j)}$ *is defined in* (3.7), *then there exists a constant* $C_1 > 0$, *such that*

$$\|w^{(j)} - u\|_a \le C_1 \zeta_a(V_H) \|u_h^{(j-1)} - u\|_a,\ j = 1, \cdots, j_h, \tag{3.10}$$

where $C_1 := \widetilde{C}_2\big(C_{e\lambda}\widetilde{C}_1 + C_{eb}\lambda\big)/c_a$, *and* $\widetilde{C}_1 > 0$, $\widetilde{C}_2 \ge 1$ *are some constants.*

Proof. From the definition (3.7), it is easy to get the following equations

$$a(w^{(j)}, v) = b(f_h^{(j)}, v) = b(\widetilde{\lambda}_h^{(j-1)}\widetilde{u}_h^{(j-1)}, v), \quad \forall v \in V.$$

It is easy to know that there exists a constant $\widetilde{C}_1 > 0$ such that $\delta_H(\lambda) \leq \widetilde{C}_1\zeta_a(V_H)$ (cf. [2, 25]). According to Theorem 2.1, (2.4) and $\zeta_a(V_h) \leq \zeta_a(V_H)$, we have

$$\begin{aligned}
\|w^{(j)} - u\|_a^2 &= a(w^{(j)} - u, w^{(j)} - u) \\
&= b(\widetilde{\lambda}_h^{(j-1)}\widetilde{u}_h^{(j-1)} - \lambda u, w^{(j)} - u) \\
&\leq \|\widetilde{\lambda}_h^{(j-1)}\widetilde{u}_h^{(j-1)} - \lambda u\|_b \|w^{(j)} - u\|_b \\
&\leq \big(|\widetilde{\lambda}_h^{(j-1)} - \lambda|\|\widetilde{u}_h^{(j-1)}\|_b + \lambda\|\widetilde{u}_h^{(j-1)} - u\|_b\big)\frac{1}{c_a}\|w^{(j)} - u\|_a \\
&\leq \frac{1}{c_a}\big(C_{e\lambda}\delta_H(\lambda) + C_{eb}\lambda\zeta_a(V_H)\big)\|\widetilde{u}_h^{(j-1)} - u\|_a\|w^{(j)} - u\|_a \\
&\leq \frac{1}{c_a}\big(C_{e\lambda}\widetilde{C}_1 + C_{eb}\lambda\big)\zeta_a(V_H)\|\widetilde{u}_h^{(j-1)} - u\|_a\|w^{(j)} - u\|_a.
\end{aligned}$$

From Ref. [2], there exists a constant $\widetilde{C}_2 \geq 1$ such that

$$\begin{aligned}
\|\widetilde{u}_h^{(j-1)} - u\|_a &\leq \widetilde{C}_2 \inf_{v_h \in V_H + \mathrm{span}\{u_h^{(j-1)}\}} \|v_h - u\|_a \\
&\leq \widetilde{C}_2\|u_h^{(j-1)} - u\|_a.
\end{aligned}$$

Combining the above two inequalities leads to

$$\begin{aligned}
\|w^{(j)} - u\|_a &\leq \frac{1}{c_a}\big(C_{e\lambda}\widetilde{C}_1 + C_{eb}\lambda\big)\zeta_a(V_H)\|\widetilde{u}_h^{(j-1)} - u\|_a \\
&\leq \frac{1}{c_a}\widetilde{C}_2\big(C_{e\lambda}\widetilde{C}_1 + C_{eb}\lambda\big)\zeta_a(V_H)\|u_h^{(j-1)} - u\|_a,
\end{aligned}$$

and we complete the proof. □

In the following lemma, we show that the iteration defined in Algorithm 3.2 can stop in finite steps and return the desired result.

Lemma 3.6. *Suppose $u_h^{(j)}$ $(0 \leq j \leq j^*, j^* \in \mathbb{N}_+)$ satisfy the loop condition in Algorithm 3.2*

$$\eta(f_h^{(j)}, u_h^{(j)}; \mathcal{T}_h) \leq \theta_2^{j+1}\zeta, \quad 0 \leq j \leq j^*, \tag{3.11}$$

where $\zeta > 0$ is the given error indicator. When H is small enough such that $C_1\zeta_a(V_H) \leq \theta_2/4$, the following property holds:

$$\|u_h^{(j)} - u\|_a \leq 2\theta_2^{j+1}C_{\mathrm{up}}\zeta + \big(C_1\zeta_a(V_H)\big)^j\|u_h^{(0)} - u\|_a, \quad 0 \leq j \leq j^*. \tag{3.12}$$

Proof. We use the mathematical induction method to give the proof. It is easy to get that (3.12) holds for $j = 0$ according to (3.9), (3.11) and Lemma 3.1. We assume (3.12) is satisfied for the case $j-1$ ($j = 1, 2, \cdots, j^*$), and we now consider the case j. From (3.7)-(3.9), Lemmas 3.1 and 3.5, we have

$$\begin{aligned}
\|u_h^{(j)} - u\|_a &\leq \|(I - P_h)w^{(j)}\|_a + \|w^{(j)} - u\|_a \\
&\leq C_{\mathrm{up}}\eta(f_h^{(j)}, u_h^{(j)}; \mathcal{T}_h) + C_1\zeta_a(V_H)\|u_h^{(j-1)} - u\|_a.
\end{aligned}$$

Together with (3.11) and the induction assumption for the case $j-1$, when H is small enough such that $C_1\zeta_a(V_H) \leq \theta_2/4$, we therefore obtain

$$\begin{aligned}
\|u_h^{(j)} - u\|_a &\leq C_{\mathrm{up}}\theta_2^{j+1}\zeta + C_1\zeta_a(V_H)\Big(2\theta_2^j C_{\mathrm{up}}\zeta + \big(C_1\zeta_a(V_H)\big)^{j-1}\|u_h^{(0)} - u\|_a\Big) \\
&\leq 2\theta_2^{j+1}C_{\mathrm{up}}\zeta + \big(C_1\zeta_a(V_H)\big)^j\|u_h^{(0)} - u\|_a.
\end{aligned}$$

Then (3.12) also holds for the case j. By the induction method, we complete the proof. □

Remark 3.3. *In this paper, we assume that the exact eigenfunction u is not a piecewise polynomial. Then we claim*

$$\exists\ j_h \in \mathbb{N}_+ \ \text{ s.t. } \ \eta(f_h^{(j_h)}, u_h^{(j_h)}; \mathcal{T}_h) > \theta_2^{j_h+1}\zeta. \tag{3.13}$$

Otherwise, according to $\theta_2 \in (0, 1)$, $C_1\zeta_a(V_H) \in (0, 1)$ and (3.12), we have $\lim_{j\to+\infty}\|u_h^{(j)} - u\|_a = 0$, which implies $u \in V_h$ and this contradicts our assumption.

3.2.2 Augmented subspace AFEM

We now proceed to propose the AFEM algorithm based on the augmented subspace method for eigenvalue problems with discontinuous coefficients. Suppose we are given an initial mesh $\mathcal{T}_H$ with mesh size H, and the corresponding finite element space V_H. $\mathcal{T}_{h_1}$ is the uniform refinement of $\mathcal{T}_H$ and the corresponding finite element space is V_{h_1}. We choose two marking parameters $\theta_1, \widehat{\theta}_1 \in (0,1)$, an error reducing ratio $\theta_2 \in (0,1)$ and a tolerance $\varepsilon > 0$.

Algorithm 3.3. ***Augmented subspace AFEM***

Input: *Given two marking parameters $\theta_1, \widehat{\theta}_1 \in (0,1)$, an error reducing ratio $\theta_2 \in (0,1)$, a tolerance $\varepsilon > 0$ and the finite element sapces V_H, V_{h_1}.*

A. Start: *Initialization.*

1. $\big[\widetilde{\lambda}_{h_1}, \widetilde{u}_{h_1}\big] = \mathsf{E\_SOLVE}(V_{h_1})$, *set* $f_{h_1} = \widetilde{\lambda}_{h_1}\widetilde{u}_{h_1}$, $f_{h_2}^{(0)} = f_{h_1}$, $u_{h_1} = \widetilde{u}_{h_1}$, $\lambda_{h_1} = \widetilde{\lambda}_{h_1}$, $n_1 = 1$, $\ell = 1$.

2. $\big[\{\eta(f_{h_1}, u_{h_1}; e)\}, \{\mathrm{osc}(f_{h_1}, u_{h_1}; \tau)\}\big] = \mathsf{ESTIMATE}(f_{h_1}, u_{h_1}, \mathcal{T}_{h_1})$, *set* $\zeta_1 = \eta(f_{h_1}, u_{h_1}; \mathcal{T}_{h_1})$.

B. Iteration: *Set $k = 2$, do the following loop until stop*

1. $\mathcal{M}_{h_{k-1}} = \mathsf{MARK}\Big(\theta_1, \widehat{\theta}_1, \{\eta(f_{h_{k-1}}, u_{h_{k-1}}; e)\}, \{\mathrm{osc}(f_{h_{k-1}}, u_{h_{k-1}}; \tau)\}, \mathcal{T}_{h_{k-1}}\Big)$;

2. $[\mathcal{T}_{h_k}, V_{h_k}] = \mathsf{REFINE}(\mathcal{M}_{h_{k-1}}, \mathcal{T}_{h_{k-1}})$;

3. $[\lambda_{h_k}, u_{h_k}, \{\eta(f_{h_k}, u_{h_k}; e)\}, \{\mathrm{osc}(f_{h_k}, u_{h_k}; \tau)\}, j_k] = \mathbf{IterAugSub}(\theta_2, V_H, V_{h_k}, \zeta_\ell, f_{h_k}^{(0)})$;

4. *(a)* **if** $j_k = 0$
set $f_{h_{k+1}}^{(0)} = f_{h_k}^{(0)}$;

(b) **else**
$\big[\widetilde{\lambda}_{h_k}, \widetilde{u}_{h_k}\big] = \mathsf{E\_SOLVE}(V_H + \mathrm{span}\{u_{h_k}\})$,
set $f_{h_{k+1}}^{(0)} = \widetilde{\lambda}_{h_k}\widetilde{u}_{h_k}$, $\zeta_{\ell+1} = \eta(f_{h_k}, u_{h_k}; \mathcal{T}_{h_k})$, $n_{\ell+1} = k$, $\ell = \ell + 1$;

5. *(a)* **if** $\eta(f_{h_k}, u_{h_k}; \mathcal{T}_{h_k}) < \varepsilon$
return (λ_{h_k}, u_{h_k});

(b) **else**
set $k = k + 1$, **goto** ***B.1***;

Output: *The desired eigenpair approximation* (λ_{h_k}, u_{h_k}).

To facilitate the understanding of Algorithm 3.3, we give the flowchart in Figure 1.

Remark 3.4. *In Algorithm 3.3, if the numerical error of the linearized problem is larger than the nonlinear error in some sense, we refine the mesh adaptively and solve the boundary value problem to reduce the corresponding numerical error. The main task in our AFEM algorithm is to solve the linearized boundary value problem, as we can prove that the nonlinear error is a higher-order term concerning the estimator, please see Theorem 4.1.*

Remark 3.5. *In Algorithm 3.3, ℓ is used for counting the number of nonzero j_k and n_ℓ documented the corresponding mesh level in which the right-hand side $f_{h_{k+1}}^{(0)}$ of the boundary value problem is newly*

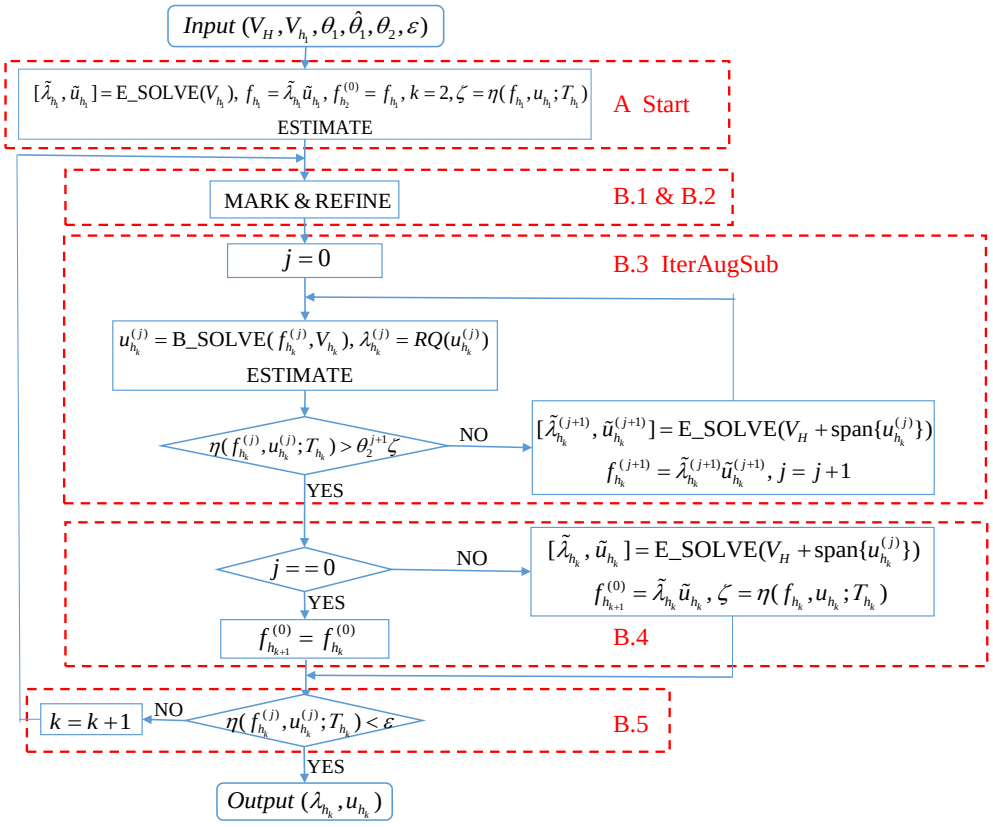

Figure 1: The flowchart of Algorithm 3.3.

defined. $j_k = 0$ *means that the numerical error of the linearized problem is somehow large in the* k*th level. Then, we do not need to change the right-hand side in the* $(k+1)$*th level.*

Similarly, define $w_k := Tf_{h_k}$, $w_k^{(j)} := Tf_{h_k}^{(j)}$, $j = 0, \cdots, j_k$, then, we have

$$u_{h_k} = P_{h_k} w_k, \quad u_{h_k}^{(j)} = P_{h_k} w_k^{(j)}, \quad j = 0, \cdots, j_k. \tag{3.14}$$

From the above relationships and the triangle inequality, it holds

$$\begin{aligned} \|u_{h_k} - u\|_a &\leq \|(I - P_{h_k})w_k\|_a + \|w_k - u\|_a, \\ \|u_{h_k}^{(j)} - u\|_a &\leq \|(I - P_{h_k})w_k^{(j)}\|_a + \|w_k^{(j)} - u\|_a, \quad j = 0, \cdots, j_k. \end{aligned} \tag{3.15}$$

According to Lemma 3.5, it is easy to show that the output of Algorithm 3.3 satisfies the following estimates.

Lemma 3.7. *There exists a positive constant* C_1 *such that the following three assertions hold*

1. *If* $k = 1$*, which means the right-hand side of the boundary value problem* $f_{h_1} = \widetilde{\lambda}_{h_1}\widetilde{u}_{h_1} = \lambda_{h_1} u_{h_1}$ *is produced by the module* E_SOLVE *in Step* ***A****.1, we have*

$$\|w_1 - u\|_a \leq C_1 \zeta_a(V_H) \|u_{h_1} - u\|_a, \tag{3.16}$$

   where C_1 *is defined in Lemma 3.5.*

2. *If* $k = n_\ell$ $(1 \neq \ell \in \mathbb{N}_+)$*, which means the right-hand side of the boundary value problem* $f_{h_k}^{(j+1)} = \widetilde{\lambda}_{h_k}^{(j)}\widetilde{u}_{h_k}^{(j)}$ $(0 \leq j < j_k)$ *is produced by the module* E_SOLVE *implicitly in Step* ***B****.3 (iterative augmented subspace method) of Algorithm 3.3, we have*

$$\|w_{n_\ell}^{(j+1)} - u\|_a \leq C_1 \zeta_a(V_H) \|u_{h_{n_\ell}}^{(j)} - u\|_a. \tag{3.17}$$

3. If $n_\ell < k \le n_{\ell+1}$ ($\ell \in \mathbb{N}_+$), which implies the right-hand side of the boundary value problem $f_{h_k}^{(0)} = \widetilde{\lambda}_{h_{n_\ell}} \widetilde{u}_{h_{n_\ell}}$ is produced by the module E_SOLVE *in Step* ***B****.4 of Algorithm 3.3, we have*

$$\|w_k^{(0)} - u\|_a \le C_1 \zeta_a(V_H) \|u_{h_{n_\ell}} - u\|_a. \tag{3.18}$$

4 Convergence of augmented subspace AFEM

We analyze the convergence of the proposed AFEM method defined by Algorithm 3.3 in this section. For this aim, we first present a preliminary result.

4.1 Preliminary result for convergence

At first, we give an important approximate property of $w_k = T f_{h_k}$, which is instrumental for the convergence analysis of the AFEM algorithm. This property means that the nonlinear error $\|w_k - u\|_a$ is a higher order term with respect to $\eta(f_{h_k}, u_{h_k}; \mathcal{T}_{h_k})$.

Theorem 4.1. *When H is small enough such that $C_1 \zeta_a(V_H) \le \theta_2/4$, the following estimate holds*

$$\|w_k - u\|_a \le C_2 \zeta_a(V_H) \eta(f_{h_k}, u_{h_k}; \mathcal{T}_{h_k}), \tag{4.1}$$

where $C_2 := \frac{4 C_1 C_{\rm up}}{\theta_2}$, and $\theta_2 \in (0,1)$.

Proof. We will use mathematical induction to carry out the proof. For the case $k = 1$, from (3.15)-(3.16), we know

$$\begin{aligned} \|w_1 - u\|_a &\le C_1 \zeta_a(V_H) \|u_{h_1} - u\|_a \\ &\le C_1 \zeta_a(V_H) \big(\|(I - P_{h_1}) w_1\|_a + \|w_1 - u\|_a \big). \end{aligned}$$

When H is small enough such that

$$C_1 \zeta_a(V_H) \le \frac{\theta_2}{4} < \frac{1}{4}, \quad \text{i.e. } C_2 \zeta_a(V_H) \le C_{\rm up}, \tag{4.2}$$

together with (3.4), we have

$$\begin{aligned} \|w_1 - u\|_a &\le \frac{C_1 \zeta_a(V_H)}{1 - C_1 \zeta_a(V_H)} \|(I - P_{h_1}) w_1\|_a \\ &\le 2 C_1 C_{\rm up} \zeta_a(V_H) \eta(f_{h_1}, u_{h_1}; \mathcal{T}_{h_1}) \\ &\le C_2 \zeta_a(V_H) \eta(f_{h_1}, u_{h_1}; \mathcal{T}_{h_1}), \end{aligned}$$

which means (4.1) holds for $k = 1$.

Now, we assume (4.1) holds for $k = n_\ell$, i.e.

$$\|w_{n_\ell} - u\|_a \le C_2 \zeta_a(V_H) \eta(f_{h_{n_\ell}}, u_{h_{n_\ell}}; \mathcal{T}_{h_{n_\ell}}). \tag{4.3}$$

Next, we will prove the desired result holds for $n_\ell < k \le n_{\ell+1}$. In the first step, we consider the case $n_\ell < k < n_{\ell+1}$. In this situation, we have $j_k = 0$, $f_{h_k} = f_{h_k}^{(0)}$, $w_k = w_k^{(0)}$ and

$$\eta(f_{h_k}^{(0)}, u_{h_k}^{(0)}; \mathcal{T}_{h_k}) > \theta_2 \zeta_\ell = \theta_2 \eta(f_{h_{n_\ell}}, u_{h_{n_\ell}}; \mathcal{T}_{h_{n_\ell}}).$$

It follows from (3.18), (3.15), (3.4), (4.3) and (4.2) that

$$\begin{aligned} \|w_k - u\|_a &\le C_1 \zeta_a(V_H) \|u_{h_{n_\ell}} - u\|_a \\ &\le C_1 \zeta_a(V_H) \big(\|(I - P_{h_{n_\ell}}) w_{n_\ell}\|_a + \|w_{n_\ell} - u\|_a \big) \\ &\le C_1 \zeta_a(V_H) \Big(C_{\rm up} + C_2 \zeta_a(V_H) \Big) \eta(f_{h_{n_\ell}}, u_{h_{n_\ell}}; \mathcal{T}_{h_{n_\ell}}) \\ &\le 2 C_1 C_{\rm up} \zeta_a(V_H) \eta(f_{h_{n_\ell}}, u_{h_{n_\ell}}; \mathcal{T}_{h_{n_\ell}}) \end{aligned}$$

$$
\begin{aligned}
&\leq \frac{2C_1C_{\rm up}}{\theta_2}\zeta_a(V_H)\eta(f_{h_k},u_{h_k};\mathcal{T}_{h_k})\\
&\leq C_2\zeta_a(V_H)\eta(f_{h_k},u_{h_k};\mathcal{T}_{h_k}).
\end{aligned}
$$

In the second step, we consider the case $k=n_{\ell+1}$. In this situation, we have $j_k>0$, $w_k=w_k^{(j_k)}$

$$
\eta(f_{h_k}^{(0)},u_{h_k}^{(0)};\mathcal{T}_{h_k})\leq\theta_2\zeta_\ell=\theta_2\eta(f_{h_{n_\ell}},u_{h_{n_\ell}};\mathcal{T}_{h_{n_\ell}}), \tag{4.4}
$$

and

$$
\eta(f_{h_k}^{(j_k)},u_{h_k}^{(j_k)};\mathcal{T}_{h_k})>\theta_2^{j_k+1}\zeta_\ell. \tag{4.5}
$$

From (3.17), (3.12) and (4.5), we have

$$
\begin{aligned}
&\|w_k^{(j_k)}-u\|_a\leq C_1\zeta_a(V_H)\|u_{h_k}^{(j_k-1)}-u\|_a\\
\leq\ & C_1\zeta_a(V_H)\Big(2\theta_2^{j_k}C_{\rm up}\zeta_\ell+\big(C_1\zeta_a(V_H)\big)^{j_k-1}\|u_{h_k}^{(0)}-u\|_a\Big)\\
\leq\ & \frac{2C_1C_{\rm up}}{\theta_2}\zeta_a(V_H)\eta(f_{h_k}^{(j_k)},u_{h_k}^{(j_k)};\mathcal{T}_{h_k})+\big(C_1\zeta_a(V_H)\big)^{j_k}\|u_{h_k}^{(0)}-u\|_a.
\end{aligned} \tag{4.6}
$$

For the last term of (4.6), combining (3.15), (3.4), (3.18), (4.4), (4.2) and (4.3), we obtain

$$
\begin{aligned}
&\|u_{h_k}^{(0)}-u\|_a\leq\|(I-P_{h_k})w_k^{(0)}\|_a+\|w_k^{(0)}-u\|_a\\
\leq\ & C_{\rm up}\eta(f_{h_k}^{(0)},u_{h_k}^{(0)};\mathcal{T}_{h_k})+C_1\zeta_a(V_H)\|u_{h_{n_\ell}}-u\|_a\\
\leq\ & C_{\rm up}\eta(f_{h_k}^{(0)},u_{h_k}^{(0)};\mathcal{T}_{h_k})+C_1\zeta_a(V_H)\big(\|(I-P_{h_{n_\ell}})w_{n_\ell}\|_a+\|w_{n_\ell}-u\|_a\big)\\
\leq\ & \theta_2C_{\rm up}\eta(f_{h_{n_\ell}},u_{h_{n_\ell}};\mathcal{T}_{h_{n_\ell}})+C_1\zeta_a(V_H)\big(C_{\rm up}+C_2\zeta_a(V_H)\big)\eta(f_{h_{n_\ell}},u_{h_{n_\ell}};\mathcal{T}_{h_{n_\ell}})\\
\leq\ & \theta_2C_{\rm up}\eta(f_{h_{n_\ell}},u_{h_{n_\ell}};\mathcal{T}_{h_{n_\ell}})+2C_1C_{\rm up}\zeta_a(V_H)\eta(f_{h_{n_\ell}};\mathcal{T}_{h_{n_\ell}})\\
\leq\ & 2\theta_2C_{\rm up}\eta(f_{h_{n_\ell}},u_{h_{n_\ell}};\mathcal{T}_{h_{n_\ell}})\\
=\ & 2\theta_2C_{\rm up}\zeta_\ell.
\end{aligned}
$$

Then, when H is small enough such that (4.2) holds, together with (4.5) we have

$$
\begin{aligned}
\big(C_1\zeta_a(V_H)\big)^{j_k}\|u_{h_k}^{(0)}-u\|_a &\leq 2\theta_2C_{\rm up}\zeta_\ell\big(C_1\zeta_a(V_H)\big)^{j_k}\\
&\leq 2\theta_2C_{\rm up}\big(C_1\zeta_a(V_H)\big)\zeta_\ell\theta_2^{j_k-1}\\
&\leq \frac{2C_1C_{\rm up}}{\theta_2}\zeta_a(V_H)\eta(f_{h_k}^{(j_k)},u_{h_k}^{(j_k)};\mathcal{T}_{h_k}).
\end{aligned} \tag{4.7}
$$

Combining (4.6) and (4.7),

$$
\begin{aligned}
\|w_k-u\|_a &= \|w_k^{(j_k)}-u\|_a\\
&\leq \frac{4C_1C_{\rm up}}{\theta_2}\zeta_a(V_H)\eta(f_{h_k}^{(j_k)},u_{h_k}^{(j_k)};\mathcal{T}_{h_k}),
\end{aligned}
$$

so (4.1) holds for $n_\ell<k\leq n_{\ell+1}$. By induction method, we complete the proof. □

4.2 Convergence of augmented subspace AFEM

The convergence theorem of our augmented subspace AFEM algorithm is given in this subsection. We first state a useful Rayleigh quotient expansion for the eigenvalue (see [2]).

Lemma 4.1. *For any $w\in V\backslash\{0\}$, we have*

$$
\frac{a(w,w)}{b(w,w)}-\widehat{\lambda}=\frac{a(w-u,w-u)}{b(w,w)}-\widehat{\lambda}\frac{b(w-u,w-u)}{b(w,w)}.
$$

Next theorem gives the convergence property of eigenpair approximation (λ_{h_k},u_{h_k}) produced by AFEM algorithm.

Theorem 4.2. *Assume the exact eigenfunction u is not a piecewise polynomial. When H is small enough such that $C_1\zeta_a(V_H) \leq \theta_2/4$, there exists a constant C_3 such that*

$$\begin{aligned} \|u_{h_k} - u\|_a &\leq C_3\beta^{(k-1)}, \quad (4.8)\\ |\lambda_{h_k} - \lambda| &\leq 2C_3^2\beta^{2(k-1)}, \quad (4.9) \end{aligned}$$

where $\max\{\sigma, \widehat{\sigma}\} < \beta < 1$, $\sigma = \left(1 - \frac{\widetilde{C}_{\text{low}}^2\theta_1^2}{2C_{\text{up}}^2\Lambda}\right)^{1/2}$, $\widehat{\sigma} = \left(1 - (1-\gamma^2)\widehat{\theta}_1^2\right)^{\frac{1}{2}}$ *are defined in Lemma 3.4,* $\gamma \in (0,1)$ *is the reduction factor defined in Remark 3.1 and* $\theta_1, \widehat{\theta}_1 \in (0,1)$ *are the refinement parameters.*

Proof. Lemmas 3.1, 3.3, 3.4 and Theorem 4.1 lead to

$$\begin{aligned} &\|u_{h_k} - u\|_a \leq \|(I - P_{h_k})w_k\|_a + \|w_k - u\|_a\\ \leq &\|(I - P_{h_k})w_k\|_a + C_2\zeta_a(V_H)\eta(f_{h_k}, u_{h_k}; \mathcal{T}_{h_k})\\ \leq &\|(I - P_{h_k})w_k\|_a + C_2\zeta_a(V_H)\frac{\Lambda^{1/2}}{C_{\text{low}}}\Big(\|(I - P_{h_k})w_k\|_a + \text{osc}(f_{h_k}, u_{h_k}; \mathcal{T}_{h_k})\Big)\\ = &\left(1 + C_2\zeta_a(V_H)\frac{\Lambda^{1/2}}{C_{\text{low}}}\right)\|(I - P_{h_k})w_k\|_a + C_2\zeta_a(V_H)\frac{\Lambda^{1/2}}{C_{\text{low}}}\text{osc}(f_{h_k}, u_{h_k}; \mathcal{T}_{h_k})\\ \leq &\left(1 + C_2\zeta_a(V_H)\frac{\Lambda^{1/2}}{C_{\text{low}}}\right)C_0\beta^{(k-1)} + C_2\zeta_a(V_H)\frac{\Lambda^{1/2}}{C_{\text{low}}}\text{osc}(f_{h_1}, u_{h_1}; \mathcal{T}_{h_1})\widehat{\sigma}^{(k-1)}. \end{aligned}$$

Notice that $\widehat{\sigma} < \beta$, then we have

$$\|u_{h_k} - u\|_a \leq C_3\beta^{(k-1)},$$

with

$$C_3 := \left(1 + C_2\zeta_a(V_H)\frac{\Lambda^{1/2}}{C_{\text{low}}}\right)C_0 + C_2\zeta_a(V_H)\frac{\Lambda^{1/2}}{C_{\text{low}}}\text{osc}(f_{h_1}, u_{h_1}; \mathcal{T}_{h_1}),$$

which is the desired result (4.8). According to the min-max principle and Lemma 4.1, we have

$$0 \leq \lambda_{h_k} - \lambda = \frac{\|u_{h_k} - u\|_a^2}{\|u_{h_k}\|_b^2} - \frac{\lambda\|u_{h_k} - u\|_b^2}{\|u_{h_k}\|_b^2} \leq \frac{\|u_{h_k} - u\|_a^2}{\|u_{h_k}\|_b^2}. \quad (4.10)$$

When H is small enough such that $\|u_{h_k} - u\|_a \leq \frac{c_a}{2}$, by (2.4) we have

$$\|u_{h_k}\|_b \geq \|u\|_b - \|u_{h_k} - u\|_b \geq 1 - \frac{1}{c_a}\|u_{h_k} - u\|_a \geq \frac{1}{2}.$$

Together with (4.10), we obtain

$$\lambda_{h_k} - \lambda \leq 2\|u_{h_k} - u\|_a^2 \leq 2C_3^2\beta^{2(k-1)},$$

which is the second desired result (4.9), and have completed the proof. □

Remark 4.1. *From the proof of Theorem 4.2, the constant C_3 will not be very large when H is small enough, that is if $H \to 0$, then $h_1 (< H) \to 0$ and $C_3 \approx C_0 \to 0$.*

5 Numerical results

In this section, two numerical examples are presented to illustrate the efficiency of the augmented subspace AFEM algorithm. In these two examples, we choose the linear Lagrange type finite element space

$$V_h = \big\{v_h \in V \ : \ v_h|_\tau \in \mathcal{P}_1(\tau), \ \ \forall \tau \in \mathcal{T}_h\big\},$$

where $\mathcal{P}_1(\tau)$ denotes the space of polynomials with degree no more than 1. The first example is used to test the efficiency of our augmented subspace AFEM, which combines the modified error estimator (3.1) with the MNS strategy. In the first example, we discuss the Laplacian eigenvalue problem with piecewise constant coefficients. In the second example, we consider a dielectric rod model of the photonic crystal eigenvalue problem. In these two examples, we choose the initial mesh as the coarsest mesh, i.e. $\mathcal{T}_{h_1} = \mathcal{T}_H$, and consequently $V_{h_1} = V_H$.

For these two examples, the exact eigenvalues are unknown, so the errors shown in the numerical tests are computed based on very accurate approximations that come from millions of DOFs. In this paper, the algorithms were implemented in Matlab (2016a) and run on a 3.00GH Intel(R) Xeon(R) Gold 6248R CPU with a 36 MB cache in Ubuntu GNU/Linux.

5.1 Eigenvalue problem with piecewise constant coefficients

In this subsection, we consider the following eigenvalue problem with piecewise constant coefficients:

$$\begin{cases} -\nabla\cdot(\alpha(\boldsymbol{x})\nabla u)+\varphi u &= \lambda u, \quad \text{in } \Omega, \\ u &= 0, \quad \text{on } \partial\Omega, \\ \int_\Omega |u|^2 \mathrm{d}\Omega &= 1, \end{cases} \tag{5.1}$$

where $\Omega = (0,1)^2$, the discontinuous coefficient

$$\alpha(\boldsymbol{x}) = \begin{cases} 100000, & \boldsymbol{x} \in (0,0.5)^2 \bigcup (0.5,1)^2, \\ 1, & \boldsymbol{x} \in (0,0.5]\times[0.5,1) \bigcup [0.5,1)\times(0,0.5], \end{cases}$$

and $\varphi = e^{(x_1-\frac{1}{2})(x_2-\frac{1}{2})}$. In this example, we test the performance of the a posteriori error estimator (3.1) and the new AFEM solver. At first, we recall the classical residual error estimator for the boundary value problem

$$\widehat{\eta}^2(f,u_h;\tau) := \|h_\tau \mathcal{R}_\tau(f,u_h)\|^2_{0,\tau} + \sum_{e\in\partial\tau} \|h_e^{1/2}\mathcal{J}_e(u_h)\|^2_{0,e}. \tag{5.2}$$

We explore the performance of three types of AFEM in this example. The first one is Algorithm 3.3, the augmented subspace AFEM with modified estimator (3.1) and MNS-marking strategy. The second one is the multilevel correction AFEM [20] with the classical estimator (5.2) and Dörfler-marking strategy (Multilevel AFEM). In this example, we set the Dörfler-marking parameter to be 0.4, the MNS-marking parameters $\theta_1 = \widehat{\theta}_1 = 0.4$, and the parameter for the augmented subspace method $\theta_2 = 0.6$.

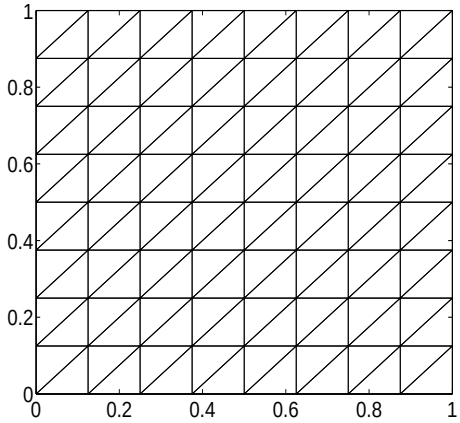

Figure 2: The initial/coarsest mesh for Example 1.

The initial mesh for this problem is shown in Figure 2. For this initial mesh, the coefficient $\alpha(\boldsymbol{x})$ is a constant on each element of the initial mesh. The meshes (the number of nodes of each method is

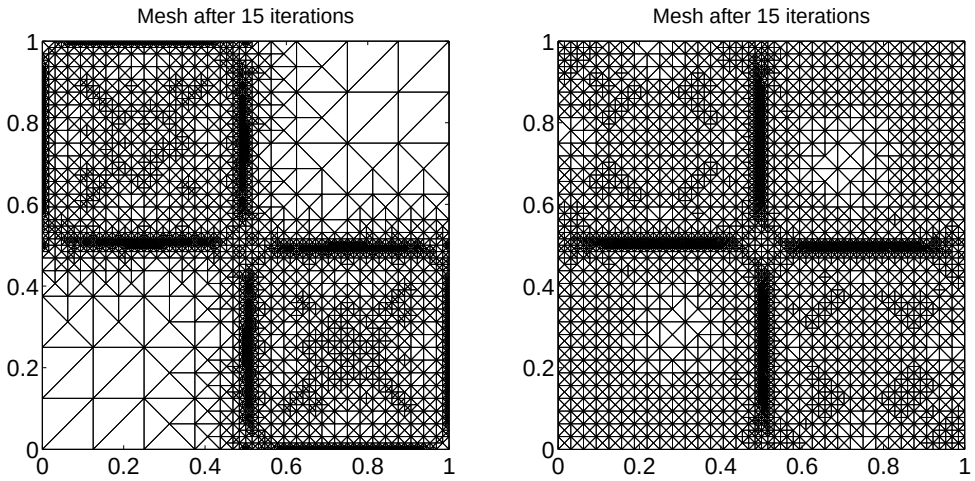

Figure 3: Meshes after 15 adaptive iterations for Algorithm 3.3 (left) and Multilevel AFEM (right).

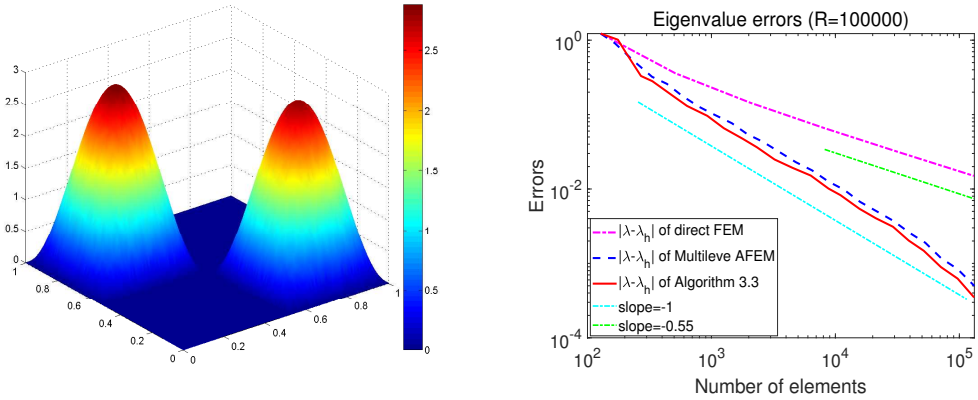

Figure 4: The eigenfunction (left) and relative error (right) of the smallest eigenvalue approximation for Example 1.

about 8500) after 15 iterations of these two types of AFEM algorithms are shown in Figure 3. Besides, the eigenfunction of problem (5.1) is given in the left subfigure of 4.

The numerical results are shown in the right subfigure of Figure 4. Due to the singularity of this problem, the convergence rate of the direct finite element method is very slow. However, these two types of AFEM algorithms achieve the optimal convergence order, and Algorithm 3.3 performs better than Multilevel AFEM.

To emphasize the high efficiency of our augmented subspace AFEM, we list j_k, the number of eigenvalue problems solved, in each iteration of Algorithm 3.3 in Table 1. From this table, we find that during the 24 adaptive iterations, we only need to solve the eigenvalue problem defined in the augmented subspaces 8 times, which reflects that our augmented subspace AFEM is more efficient than multilevel correction AFEM [20].

Table 1: The number of eigenvalue problem solving in Algorithm 3.3 for Example 1.

k	1	2	3	4	5	6	7	8	9	10	11	12
j_k	0	2	0	1	0	0	1	0	0	1	0	0
k	13	14	15	16	17	18	19	20	21	22	23	24
j_k	0	1	0	0	0	1	0	0	0	1	0	0

5.2 An example in photonic crystal

In this subsection, we consider an example of a photonic crystal. Photonic crystals are periodic fine structures composed of different dielectric materials. Under some assumptions, the propagation of light in photonic crystals can be described by a cluster of eigenvalue problems with periodic boundary conditions. In this example, we consider the following transverse electric (TE) mode:

$$-(\nabla + \mathrm{i}\kappa) \cdot \Big(\frac{1}{\varepsilon}(\nabla + \mathrm{i}\kappa)u\Big) = \lambda\, u \quad \text{in } \Omega, \tag{5.3}$$

where $\Omega = (-0.5, 0.5)^2$, $\mathrm{i} = \sqrt{-1}$, $\kappa \in (-\pi, \pi)^2$ is the quasimomentum, ε is the dielectric permittivity and defined as

$$\varepsilon = \begin{cases} 1 \quad \text{(air)}, & \text{in } (-0.25, 0.25)^2, \\ 20 \text{ (dielectric material)}, & \text{in } \Omega \backslash (-0.25, 0.25)^2, \end{cases}$$

(see the left subfigure of Figure 5, and the "dark region" represents "dielectric material"). Actually, this is a realistic situation, for example, the permittivity of Silicon is 11.7, and Gallium Arsenide (GaAs) is 13.18.

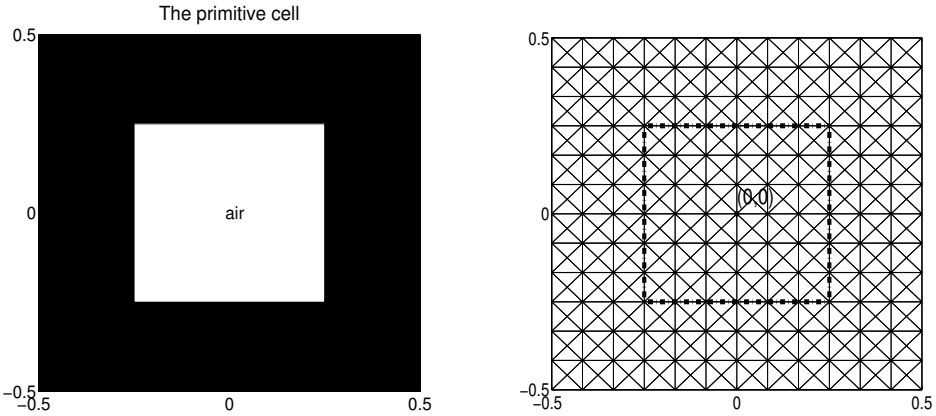

Figure 5: The primitive cell Ω (left) and its initial/coarsest mesh (right) for Example 2.

In this example, we choose $\theta_1 = \widehat{\theta}_1 = 0.3$, $\theta_2 = 0.5$. Considering the periodic boundary condition, we choose a kind of symmetric mesh aligned with the jumps of the dielectric permittivity (the coefficient ε is a constant on each element) as the initial mesh. The initial mesh for this example is shown in the right subfigure of Figure 5.

The left subfigure of Figure 6 gives the adaptively refined meshes for $\kappa = (0, 0)$ which corresponds to T in the left subfigure of Figure 10. The eigenfunction of **the smallest nonzero eigenvalue** for $\kappa = (0, 0)$ is shown in the right subfigure of Figure 6, which corresponds to the red star marker on the second band function in the right subfigure of Figure 10. The numerical results of Algorithm 3.3 for this example with $\kappa = (0, 0)$ are given in Figure 7, in which we find that Algorithm 3.3 obtains the optimal convergence rate.

Similarly to Example 1, we give the number of eigenvalue problem-solving (j_k) in each iteration of Algorithm 3.3 in Table 2. During the 24 adaptive iterations, we only need to solve the eigenvalue problem defined in the augmented subspaces 5 times in this example. These data strongly demonstrate the efficiency of our algorithm.

Table 2: The number of eigenvalue problem solving in Algorithm 3.3 for Example 2 with $\kappa = (0, 0)$.

k	1	2	3	4	5	6	7	8	9	10	11	12
j_k	0	1	0	0	0	1	0	0	0	0	1	0
k	13	14	15	16	17	18	19	20	21	22	23	24
j_k	0	0	0	1	0	0	0	0	1	0	0	0

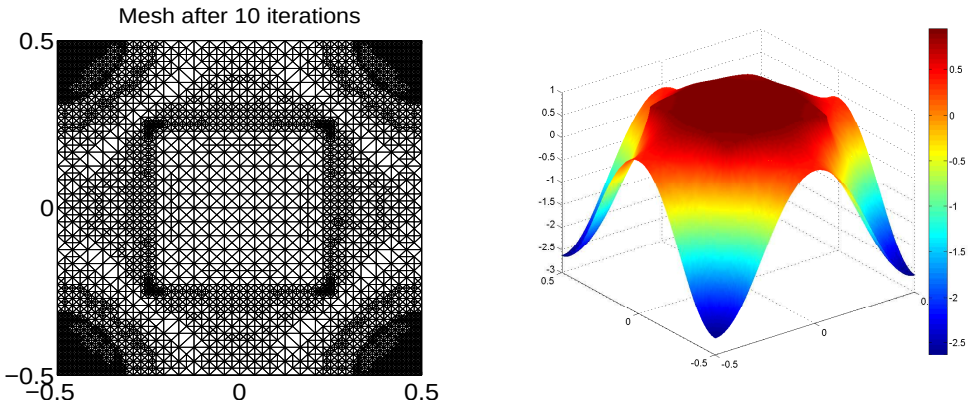

Figure 6: Mesh after 10 adaptive iterations (left) and the eigenfunction (right) with $\kappa = (0, 0)$ for Example 2.

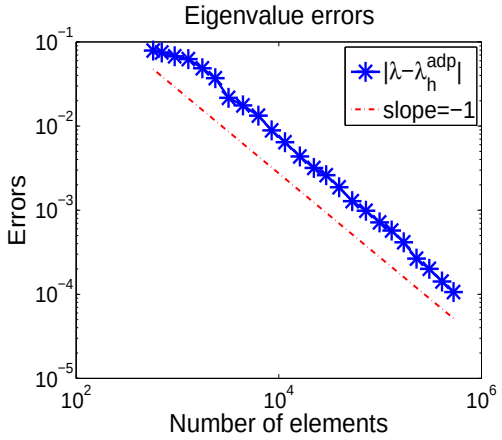

Figure 7: The error of the smallest non-zero eigenvalue for Example 2 with $\kappa = (0, 0)$.

Besides, we also show the numerical result for $\kappa = (\pi/2, 0)$, which corresponds to S in the left subfigure of Figure 10. The adaptively refined mesh and eigenfunction are given in Figure 8. The numerical results are shown in Figure 9, which corresponds to the blue star marker on the first band function in the right subfigure of Figure 10. And the number of eigenvalue problem solving j_k is listed in Table 3, which also demonstrates the high efficiency of Algorithm 3.3.

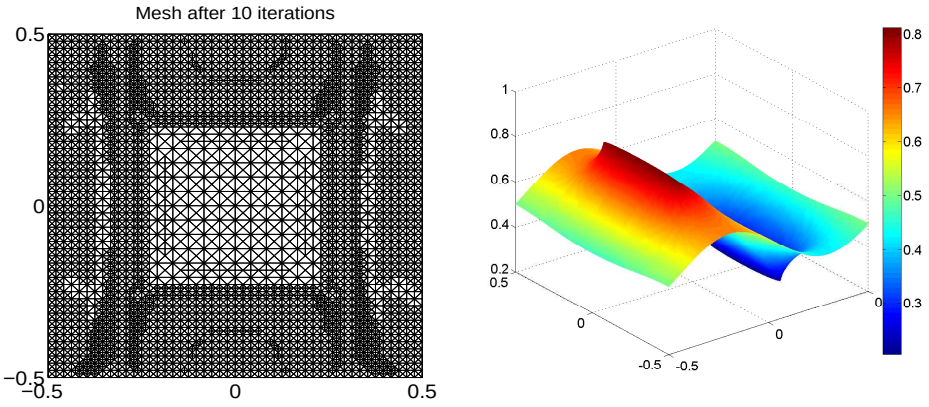

Figure 8: Mesh after 10 adaptive iterations (left) and the eigenfunction (right) for Example 2 with $\kappa = (\pi/2, 0)$.

The band structure of this model is also discussed. Calculations of band gaps can be carried out

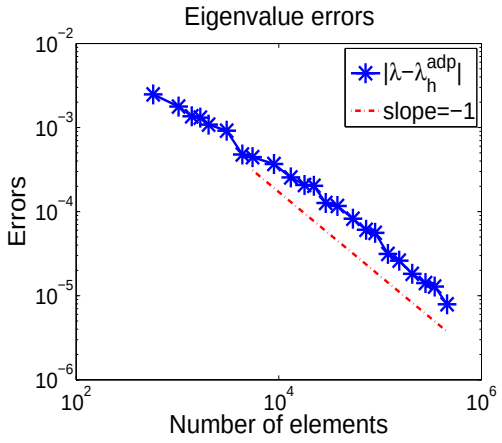

Figure 9: The error of the smallest non-zero eigenvalue for Example 2 with $\kappa = (\pi/2, 0)$.

Table 3: The number of eigenvalue problem solving in Algorithm 3.3 for Example 2 with $\kappa = (\pi/2, 0)$.

k	1	2	3	4	5	6	7	8	9	10	11	12
j_k	0	1	0	0	0	1	0	0	0	1	0	0
k	13	14	15	16	17	18	19	20	21	22	23	24
j_k	0	1	0	0	0	1	0	0	0	1	0	0

just along the boundary of the irreducible Brillouin zone [32,36] (see the left subfigure in Figure 10). The mirror symmetry makes this possible. The union set of the spectra of problem (5.3) with κ along the boundary of the reduced Brillouin zone contains all the spectra of this PC eigenvalue problem. There exists an eigenvector for each eigenvalue, and each eigenvector represents a mode propagating through the PC. So the non-spectrum interval means no wave with these frequencies can propagate in the PC, and we call it a band gap.

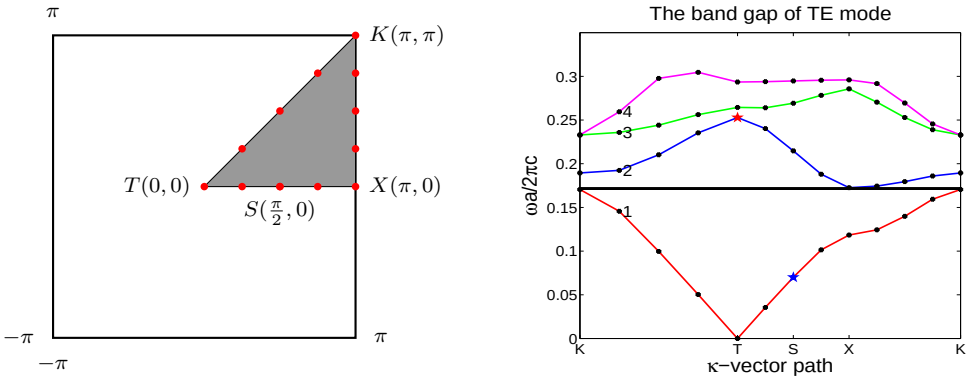

Figure 10: Irreducible Brillouin zone (the dark triangle KTX) (left) and the first four band functions (dispersion relations) (right) for Example 2.

The right subfigure in Figure 10 shows graphs of the first four band functions (dispersion relations). As is customary in physics, these band functions are drawn using the eigenvalues of problem (5.3) with quasimomentum parameter κ taking the following values (on the boundary of the irreducible Brillouin zone): $K(\pi, \pi)$, $(3\pi/4, 3\pi/4)$, $(\pi/2, \pi/2)$, $(\pi/4, \pi/4)$, $T(0, 0)$, $(\pi/4, 0)$, $S(\pi/2, 0)$, $(3\pi/4, 0)$, $X(\pi, 0)$, $(\pi, \pi/4)$, $(\pi, \pi/2)$, $(\pi, 3\pi/4)$, see Figure 10. The y-coordinate denotes the frequencies in the dimensionless unit $\omega a/2\pi c = \sqrt{\lambda}a/2\pi$. From the right subfigure in Figure 10, we know that there exists a big band gap between the first two bands.

6 Concluding remarks

We have designed an augmented subspace AFEM for eigenvalue problems with discontinuous coefficients and analyzed the convergence of this algorithm. The main idea of this AFEM algorithm is: when the linear error (numerical error of the linearized boundary value problem) is larger than the nonlinear error (the error between solutions of linearized boundary value problem and eigenvalue problem) in some sense, we use the new a posteriori error estimator to refine the mesh adaptively, and then solve the boundary value problem on the adaptively refined mesh to reduce the linear error; otherwise, we solve an eigenvalue problem on a very low-dimensional augmented subspace and update the right-hand side of the boundary value problem to reduce the nonlinear error. Hence, our algorithm evidently improves the solving efficiency. The idea and method here can be extended to other eigenvalue problems with discontinuous coefficients, such as the Maxwell eigenvalue problem and the Stokes eigenvalue problem.

Acknowledgements

The authors would like to thank the reviewers for their valuable comments and helpful suggestions that improved this paper. M. Xie was partially supported by the National Natural Science Foundation of China (No. 12001402, 12271400, 12571437). M. Yue was partially supported by the National Natural Science Foundation of China (No. 12201017).

References

[1] L.E. Andersson, *Inverse eigenvalue problems with discontinuous coefficients*, Inverse problems, 4(2) (1988), pp. 353–397.

[2] I. Babuška and J. Osborn, *Finite element-Galerkin approximation of the eigenvalues and eigenvectors of selfadjoint problems*, Math. Comp., 52(186) (1989), pp. 275–297.

[3] I. Babuška and J. Osborn, *Eigenvalue Problems*, In Handbook of Numerical Analysis, Vol. II, (Eds. P. G. Lions and Ciarlet P.G.), Finite Element Methods (Part 1), North-Holland, Amsterdam, 1991, pp. 641–787.

[4] R.E. Bank, L. Grubišić and J. Ovall, *A framework for robust eigenvalue and eigenvector error estimation and Ritz value convergence enhancement*, Appl. Numer. Math., 66 (2012), pp. 1–29.

[5] J. Bielak, *Some remarks on bounds to eigenvalues of Sturm-Liouville problems with discontinuous coefficients*, Z. Angew. Math. Phys., 32 (1981), pp. 647–657.

[6] D. Boffi, M. Conforti and L. Gastaldi, *Modified edge finite elements for photonic crystals*, Numer. Math., 105(2) (2006), pp. 249–266.

[7] S.C. Brenner and L.R. Scott, *The mathematical theory of finite element methods*, Texts in Applied Mathematics, vol. 15, Springer-Verlag, New York, 1994.

[8] A. Buffa and I. Perugia, *Discontinuous Galerkin approximation of the Maxwell eigenproblem*, SIAM J. Numer. Anal., 44(5) (2006), pp. 2198–2226.

[9] H. Chen, L. He, A. Zhou, *Finite element approximations of nonlinear eigenvalue problems in quantum physics*, Comput. Methods Appl. Mech. Engrg., 200(21) (2011), pp. 1846–1865.

[10] J. Chen, Y. Li, and X. Hu, *A two-grid method for the phase-field model of photonic band gap optimization*, Comput. Math. Appl., 96 (2021), pp. 44–54.

[11] Z. Chen and S. Dai, *On the efficiency of adaptive finite element methods for elliptic problems with discontinuous coefficients*, SIAM J. Sci. Comput., 24(2) (2002), pp. 443–462.

[12] P.G. Ciarlet, *The finite element method for elliptic problem*, North-holland Amsterdam, 1978.

[13] M. Dryja, M. Sarkis and O. Widlund, *Multilevel Schwarz methods for elliptic problems with discontinuous coefficients in three dimensions*, Numer. Math., 72 (1996), pp. 313–348.

[14] C. Engwer, P. Henning, A. Målqvist and D. Peterseim, *Efficient implementation of the localized orthogonal decomposition method*, Comput. Methods Appl. Mech. Engrg., 350(15) (2019), pp. 123–153.

[15] S. Giani and I.G. Graham, *Adaptive finite element methods for computing band gaps in photonic crystals*, Numer. Math., 121(1) (2012), pp. 31–64.

[16] S. Giani, L. Grubišić, L. Heltai and O. Mulita, *Smoothed-adaptive perturbed inverse iteration for elliptic eigenvalue problems*, Comput. Methods Appl. Math., 21(2) (2021), pp. 385–405.

[17] S. Giani and P. Šolín, *Solving elliptic eigenproblems with adaptive multimesh hp-FEM*, J. Comput. Appl. Math., 394 (2021), pp. 113528.

[18] S. Guo, D. Li, H. Feng and X. Lu, *Extremal eigenvalues of the Sturm-Liouville problems with discontinuous coefficients*, Numer. Math. Theory Methods Appl., 6(4) (2013), pp. 657–684.

[19] P. Henning, A. Målqvist and D. Peterseim, *Two-Level discretization techniques for ground state computations of Bose-Einstein condensates*, SIAM J. Numer. Anal., 52(4) (2014), pp. 1525–1550.

[20] Q. Hong, H. Xie and F. Xu, *A multilevel correction type of adaptive finite element method for eigenvalue problems*, SIAM J. Sci. Comput., 40(6) (2018), pp. A4208–A4235.

[21] G. Hu, H. Xie and F. Xu, *A multilevel correction adaptive finite element method for Kohn-Sham equation*, J. Comput. Phys., 355 (2018), pp. 436–449.

[22] S. Jia, H. Xie, M. Xie and F. Xu, *A full multigrid method for nonlinear eigenvalue problems*, Sci. China Math., 59 (2016), pp. 2037–2048.

[23] D. Klindworth and K. Schmidt, *An efficient calculation of photonic crystal band structures using Taylor expansions*, Commun. Comput. Phys., 16(5) (2014), pp. 1355–1388.

[24] Q. Lin and H. Xie, *A multi-level correction scheme for eigenvalue problems*, Math. Comp., 84(291) (2015), pp. 71–88.

[25] Q. Lin, H. Xie and J. Xu, *Lower bound of the discretization error for piecewise polynomials*, Math. Comp., 83(285) (2014), pp. 1–13.

[26] Z. Lu, A. Cesmelioglu, J.J.W. Van der Vegt and Y. Xu, *Discontinuous Galerkin approximations for computing electromagnetic Bloch modes in photonic crystals*, J. Sci. Comput., 70 (2017), pp. 922–964.

[27] J. Maubach, *Local bisection refinement for n-simplicial grids generated by reflection*, SIAM J. Sci. Comput., 16 (1995), pp. 210–227.

[28] K. Mekchay and R.H. Nochetto, *Convergence of adaptive finite element methods for general second order linear elliptic PDEs*, SIAM J. Numer. Anal., 43 (2005), pp. 1803–1827.

[29] M.S. Min and D. Gottlieb, *Domain decomposition spectral approximations for an eigenvalue problem with a piecewise constant coefficient*, SIAM J. Numer. Anal., 43 (2005), pp. 502–520.

[30] P. Morin, R.H. Nochetto and K.G. Siebert, *Data oscillation and convergence of adaptive FEM*, SIAM J. Numer. Anal., 38 (2000), pp. 466–488.

[31] P. Morin, R.H. Nochetto and K.G. Siebert, *Convergence of adaptive finite element methods*, SIAM Rev., 44 (2002), pp. 631–658.

[32] E. Moreno, D. Erni and C. Hafner, *Bandstructure computations of metallic photonic crystals with the multiple multipole method*, Phys. Rev. B, 65(15) (2002), pp. 155120.

[33] K. Neymeyr, *A posteriori error estimation for elliptic eigenproblems*, Numer. Linear Algebra Appl., 9(4) (2002), pp. 263–279.

[34] M. Petzoldt, Regularity and error estimators for elliptic problems with discontinuous coefficients, Weierstraß-Institut, 2001.

[35] M. Petzoldt, A Posteriori Error Estimators for Elliptic Equations with Discontinuous Coefficients, Adv. Comput. Math., 16(1) (2002), pp. 47–75.

[36] K. Schmidt and P. Kauf, *Computation of the band structure of two-dimensional photonic crystals with hp finite elements*, Comput. Methods Appl. Mech. Engrg., 198(13) (2009), pp. 1249–1259.

[37] P. Šolín and S. Giani, An iterative adaptive finite element method for elliptic eigenvalue problems, J. Comput. Appl. Math., 236(18) (2012), pp. 4582–4599.

[38] C.T. Traxler, *An algorithm for adaptive mesh refinement in n dimensions*, Computing, 59 (1997), pp. 115–137.

[39] L. Wang, Z. Xie and Z. Zhang, *Super-geometric convergence of a spectral element method for eigenvalue problems with jump coefficients*, J. Comput. Math., 28(3) (2010), pp. 418–428.

[40] W. Xiao, B. Gong, J. Sun and Z. Zhang, *Finite element calculation of photonic band structures for frequency dependent materials*, J. Sci. Comput., 87 (2021), pp. 27.

[41] H. Xie, *A multigrid method for eigenvalue problem*, J. Comput. Phys., 274 (2014), pp. 550–561.

[42] J. Xu, *Iterative methods by space decomposition and subspace correction*, SIAM Rev., 34(4) (1992), pp. 581–613.

[43] J. Xu and A. Zhou, *A two-grid discretization scheme for eigenvalue problems*, Math. Comp., 70(233) (1999), pp. 17–25.

[44] M. Yue, H. Xie and M. Xie, *Augmented Subspace Adaptive Finite Element Method for Computing Band Gaps of Photonic Crystals*, finished.